

DEPENDENCIES BETWEEN CODING GAIN AND FILTER LENGTH IN PARAUNITARY FILTER BANKS DESIGNED USING QUATERNIONIC APPROACH

Marek Parfieniuk and Alexander Petrovsky

Department of Real-Time Systems, Bialystok Technical University
Wiejska 45A street, 15-351 Bialystok, Poland
phone: + (48 85) 746-90-50, fax: + (48 85) 746-90-57
email: marekpk@wi.pb.edu.pl, palex@it.org.by

ABSTRACT

In this paper, we investigate the performance limits of four-channel paraunitary filter banks designed using quaternionic approach. Our aim is to reveal how the maximum achievable coding gain depends on the filter length, linearity of the phase responses, and system one-regularity. We also try to obtain some additional insight into coefficient synthesis for paraunitary filter banks, which is often a difficult optimization problem. The results may provide useful advice for the designers who intend to employ filter banks in subband image coding as well as in other applications.

1. INTRODUCTION

It is not easy to evaluate how a filter bank performs in signal compression. Although the coding gain is mainly used for these purposes, it should not be considered separately from other characteristics of the system.

Firstly, the coding gain can easily be calculated only if the filters are orthogonal [1, 2]. This is the reason for the great importance of paraunitary filter banks (PUFBs), even though the biorthogonal ones have advantages of improved design flexibility and the independence of perfect reconstruction from computational accuracy.

Secondly, other properties of the system affect the perceived quality of the signal reconstructed from quantized subband samples. These are the linearity of the phase responses and the regularity of the wavelet basis. Each of these properties also restricts the design freedom to be exploited in the maximization of the coding gain.

Finally, the coding gain depends on the filter length and number of subbands. As these parameters are directly related to the computational complexity of the filter bank, design trade-offs are unavoidable.

Obviously, such important questions have already been addressed [1, 2, 3, 4]. In spite of that, good reasons motivated us to do some research on the coding gain of PUFBs.

First of all, we have recently developed quaternionic lattice structures for 4- and 8-channel, general and linear phase (LP) PUFBs, also those with pairwise-mirror-image (PMI) symmetric magnitude responses. Our approach differs from the conventional ones in the structural imposition of losslessness, so that systems implemented in finite-precision arithmetic remain paraunitary. Moreover, the one-regularity conditions lucidly expressed using hypercomplex lattice coefficients are very practical from the point of view of implementation. In this paper, we would like to prove that the method is a good tool for the coefficient synthesis itself and to determine the relations between the coding gain and filter length for the developed quaternionic factorizations. Persons who intend to use these filter banks might appreciate clear tables and plots that show the achievable coding performance limits and thus facilitate design. The authors did not notice such data for PMI and one-regular PUFBs in the literature.

On the other hand, coefficient synthesis for perfect reconstruction filter banks is usually only briefly outlined, without going into

details about the nature of the related problem of numerical optimization and the methods of solution. So, we decide to reveal a simple procedure which gives good results and might be helpful for other people who contend with similar problems.

The organization of the paper is as follows. In Section 2, the reader is briefly acquainted with the factors that determine the coding performance of a paraunitary filter bank. Then, quaternionic lattice structures for 4-channel PUFBs are presented in Section 3. For brevity and coherence, we omit 8-channel filter banks from this paper, but we intend to consider them in a future work. Section 4 discusses coefficient synthesis as a numerical optimization problem and presents our approach. The experimental results are shown in Section 4 with thorough comments. Then, the conclusions are drawn in the last section.

Notations: Column vectors are denoted by lower-case bold-faced characters, whereas matrices by the upper-case ones. The notation $[A]_{mn}$ refers to the (m, n) entry of a matrix A . I_m and J_m denote the $m \times m$ identity and reverse identity matrices, respectively. The superscript T stands for transposition.

2. CODING PERFORMANCE OF PUFBs

2.1 Coding gain

The most essential performance measure for an M -band PUFB used in data compression is the coding gain defined by [2]

$$CG = 10 \log_{10} \frac{\frac{1}{M} \sum_{k=0}^{M-1} \sigma_{x_k}^2}{\left(\prod_{k=0}^{M-1} \sigma_{x_k}^2 \right)^{\frac{1}{M}}}. \quad (1)$$

The subband variances $\sigma_{x_k}^2$ correspond to the diagonal elements of the autocorrelation matrix of the transformed signal, so they can be calculated as

$$\sigma_{x_k}^2 = [\mathbf{H} \mathbf{R}_{xx} \mathbf{H}^T]_{kk}. \quad (2)$$

To determine the product in the square brackets, which represents that matrix, we need the autocorrelation matrix \mathbf{R}_{xx} of the input signal as well as the transform matrix \mathbf{H} that describes the filter bank.

The transform matrix is formed from the impulse response coefficients as follows:

$$[\mathbf{H}]_{kn} = h_k(L-1-n), \quad (3)$$

where $k = 0, \dots, M-1$ and $n = 0, \dots, L-1$, assuming that the filters are of length L .

In our experiments, the matrix \mathbf{R}_{xx} was generated for an AR(1) input process with unit variance and the correlation coefficient of 0.95. Such a model is particularly appropriate only for natural images, and therefore other applications will require different approaches.

It should be emphasized that both (1) and (2) are valid only for PUFBs. The analysis of biorthogonal filter banks is more difficult because of correlations between their subbands [1].

In spite of its theoretical foundations, the coding gain is a good predictor of experimental rate-distortion performance of filter banks [3]. In image compression, however, its high value should be accompanied by additional properties of the system.

2.2 Linearity of phase responses

Linear phase responses of a filter bank are necessary to use symmetric extension to handle the boundaries of finite-length signals such as images. Unlike other approaches for obtaining nonexpansive transforms, this kind of extension does not introduce discontinuities into data and thus does not cause high-frequency artifacts [5].

2.3 Regularity and DC Leakage

It is desirable to approximate smooth signals using basis functions that have the same property. In coding, this prevents blocking artifacts [5]. That is why regular filter banks that generate smooth wavelet bases are developed.

For an M -band filter bank, regularity can be defined as the number of zeros at the mirror (aliasing) frequencies $2k\pi/M, k = 1, \dots, M-1$ of the lowpass filter $H_0(z)$. To obtain K degrees of regularity, the polyphase matrix $\mathbf{E}(z)$ must satisfy the condition [6]

$$\frac{d^n}{dz^n} \left\{ \mathbf{E}(z^M) \begin{bmatrix} 1 & z^{-1} & \dots & z^{-(M-1)} \end{bmatrix}^T \right\} \Big|_{z=1} = c_n \mathbf{e}, \quad (4)$$

where $\mathbf{e} = [1 \ 0 \ \dots \ 0]^T$, and $c_n \neq 0$ for $n = 0, \dots, K-1$.

The one-regularity ($K = 1$) is of essential importance as its absence causes DC leakage, which is visible as the particularly annoying checkerboard artifact in decoded images.

3. QUATERNIONIC APPROACH TO 4-CHANNEL PUFBS

3.1 Quaternions

Quaternions discovered by Hamilton in 1843 are hypercomplex numbers of the form [7]

$$q = q_1 + q_2i + q_3j + q_4k, \quad q_1, q_2, q_3, q_4 \in \mathbb{R}, \quad (5)$$

with one real and three distinct imaginary parts. The imaginary units: i, j , and k are related by the following equations:

$$\begin{aligned} i^2 = j^2 = k^2 = ijk = -1, \\ ij = -ji = k, \quad jk = -kj = i, \quad ki = -ik = j, \end{aligned} \quad (6)$$

so quaternion multiplication is non-commutative. However, the conjugate

$$\bar{q} = q_1 - q_2i - q_3j - q_4k, \quad (7)$$

the norm (modulus)

$$|q| = \sqrt{q\bar{q}} = \sqrt{\bar{q}q} = \sqrt{q_1^2 + q_2^2 + q_3^2 + q_4^2}, \quad (8)$$

and other operations are defined similarly as in the case of ordinary complex numbers.

3.2 Quaternion multiplication matrices

Because quaternions can be identified with four-element column vectors:

$$q \Leftrightarrow \mathbf{q} = [q_1 \ q_2 \ q_3 \ q_4]^T, \quad (9)$$

it is possible to represent hypercomplex arithmetic operations in vector-matrix notation. In particular, the multiplication can be writ-

ten as

$$pq \Leftrightarrow \underbrace{\begin{bmatrix} p_1 & -p_2 & -p_3 & -p_4 \\ p_2 & p_1 & -p_4 & p_3 \\ p_3 & p_4 & p_1 & -p_2 \\ p_4 & -p_3 & p_2 & p_1 \end{bmatrix}}_{\mathbf{M}^+(p)} \times \begin{bmatrix} q_1 \\ q_2 \\ q_3 \\ q_4 \end{bmatrix} \quad (10a)$$

$$= \underbrace{\begin{bmatrix} q_1 & -q_2 & -q_3 & -q_4 \\ q_2 & q_1 & q_4 & -q_3 \\ q_3 & -q_4 & q_1 & q_2 \\ q_4 & q_3 & -q_2 & q_1 \end{bmatrix}}_{\mathbf{M}^-(q)} \times \begin{bmatrix} p_1 \\ p_2 \\ p_3 \\ p_4 \end{bmatrix}, \quad (10b)$$

using one of two multiplication matrices: the left- $\mathbf{M}^+(\cdot)$ or right-operand $\mathbf{M}^-(\cdot)$ one. Both matrices are orthogonal, or orthonormal if the quaternions have unit norm. Owing to their idiosyncratic structures, the matrices are very useful in diverse scientific applications.

3.3 Quaternion multiplier as a paraunitary building block

We have proposed to use quaternion multiplication matrices in factorizations for 4- and 8-channel PUFBS [8, 9, 10, 11]. Unlike the conventional counterparts, the lattice structures with hypercomplex multipliers in the role of an essential building block always give orthogonal filters, even if the multiplier coefficients are quantized.

To represent quaternion multipliers in schemes, we have also introduced the symbols shown in Figure 1.

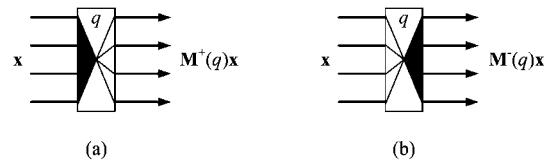


Figure 1: Graphical symbols for quaternion multipliers whose coefficient q is (a) the left- and (b) right-hand factor, respectively.

3.4 Four-channel general PUFB

The filters of a general PUFB satisfy no other constraints apart from orthogonality. The quaternionic factorization of the polyphase matrix $\mathbf{E}(z)$ of such a 4-channel system has the following form [8]:

$$\mathbf{E}(z) = \mathbf{G}_{N-1}(z) \mathbf{G}_{N-2}(z) \dots \mathbf{G}_1(z) \mathbf{E}_0, \quad (11)$$

of the cascade of N stages, where

$$\mathbf{E}_0 = \mathbf{M}^+(q_0) \mathbf{M}^-(p_0), \quad (12)$$

and

$$\mathbf{G}_i(z) = \mathbf{M}^\pm(q_i) \text{diag} \left(z^{-1}, \mathbf{I}_{M-1} \right), \quad i = 1, \dots, N-1, \quad (13)$$

where p_0 and all q_i are unit-norm quaternions. For $N = 3$, the corresponding lattice structure is shown in Figure 2(a).

The design freedom is related only to the hypercomplex coefficients, although the factors in (12) can be ordered arbitrarily, and (13) can be based on both left- and right-operand quaternion multiplication matrices.

Assuming that the left-operand multiplication matrix is used in (13), the above factorization gives a one-regular filter bank iff

$$p_0 = \pm \frac{1}{2} \overline{o q_{N-1} \dots q_0}, \quad (14)$$

where $o = 1 + i + j + k$.

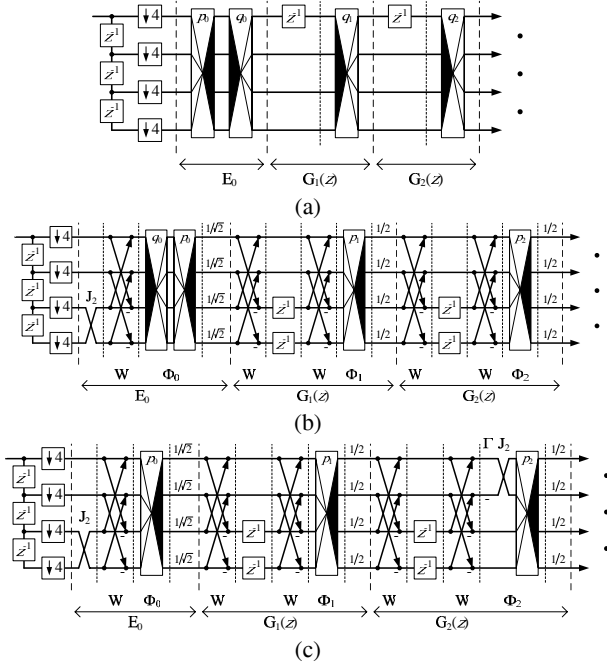


Figure 2: Quaternionic lattice structures for 4-channel (a) general, (b) LP, and (c) PMI LP PUFBs ($N = 3$).

3.5 Four-channel LP PUFB

The polyphase matrix of a 4-channel LP PUFB can also be factorized according to (11), but the definitions of the stages are different. Namely [8],

$$E_0 = \frac{1}{\sqrt{2}} \Phi_0 W \text{diag} \left(I_{M/2}, J_{M/2} \right), \quad (15)$$

and

$$G_i(z) = \frac{1}{2} \Phi_i W \text{diag} \left(I_{M/2}, z^{-1} I_{M/2} \right) W, \quad i = 1, \dots, N-1, \quad (16)$$

where

$$W = \begin{bmatrix} I_{M/2} & I_{M/2} \\ I_{M/2} & -I_{M/2} \end{bmatrix}, \quad (17)$$

$$\Phi_0 = M^-(p_0) M^+(q_0), \quad (18)$$

and

$$\Phi_i = M^-(p_i), \quad i = 1, \dots, N-1. \quad (19)$$

All p_i and q_0 are unit quaternions that have the two last imaginary parts (related to j and k) set to zero. So the coefficients are unit complex numbers in fact. For $N = 3$, the corresponding lattice structure is shown in Figure 2(b).

A filter bank described by such a factorization is one-regular iff

$$q_0 = \pm \frac{1}{\sqrt{2}} p_0 \cdots p_{N-1} \bar{a}, \quad (20)$$

where $a = 1 + i$.

3.6 Four-channel PMI LP PUFB

To have pairwise-mirror-image symmetric magnitude responses, it is sufficient to take

$$\Phi_i = M^-(p_i), \quad i = 0, \dots, N-2, \quad (21)$$

and

$$\Phi_{N-1} = M^-(p_{N-1}) \text{diag} (J_2 \Gamma, I_2), \quad (22)$$

where $\Gamma = \text{diag} (1, -1)$, in the factorization presented in Section 3.5 [8]. For $N = 3$, the corresponding lattice structure is shown in Figure 2(c).

The quaternionic coefficients p_i are again restricted to be unit complex numbers. A filter bank realized using this approach is one-regular iff

$$p_{N-1} = \pm \frac{1}{\sqrt{2}} a p_0 \cdots p_{N-2}, \quad (23)$$

where a is defined as in (20).

4. METHOD OF COEFFICIENT SYNTHESIS

Our design goal is to obtain the coefficients which maximize the coding gain of the filter bank realized using a given factorization.

To ensure that hypercomplex coefficients have unit norm, optimization can be performed indirectly, by using the polar form of a quaternion

$$\begin{aligned} q_1 &= |q| \cos \phi, \\ q_2 &= |q| \sin \phi \cos \psi, \\ q_3 &= |q| \sin \phi \sin \psi \cos \chi, \\ q_4 &= |q| \sin \phi \sin \psi \sin \chi, \end{aligned} \quad (24)$$

which is much more convenient to deal with than real and imaginary parts. All quaternions of a given norm can simply be produced by changing the values of ϕ , ψ , and χ . The minimum ranges of the angles necessary to cover a particular subset of hypercomplex numbers are mutually dependent and can be selected in numerous ways. For example $0 \leq \phi < 2\pi$, $0 \leq \psi \leq \pi$, and $0 \leq \chi \leq \pi$ are sufficient to obtain an arbitrary quaternion. Complex numbers are then obtained by taking $\psi = 0$, which makes χ meaningless and ϕ deciding.

In this way, we can make the coding gain a function of a vector of angles, each of which is one degree of design freedom. Every three elements of the vector describe one coefficient of the lattice structure for general PUFBs. In the case of (PMI) LP PUFBs, there is a one-to-one correspondence between an angle and degenerated hypercomplex coefficient. The calculation of the objective function for given angle values comprises the conversion of the coefficients from their polar to rectangular form, generation of the polyphase matrix according to the appropriate factorization, assembling the transform matrix, and using it in (2).

Due to the periodicity of trigonometric functions, it is unnecessary to constrain the angles, so their values that maximize the coding gain can be searched using efficient algorithms for unconstrained optimization. We tested both `fminunc` and `fminsearch` routines provided by MATLAB to solve such problems [12]. Whereas `fminsearch` uses the simplex search method, `fminunc` uses the quasi-Newton method with numerical gradient approximation. Both are sensitive to the selection of the starting point and do not guarantee to locate the global maximum. So advanced problems require repeating the optimization for a number of different starting points, and using different methods to verify the obtained results.

5. EXPERIMENTAL RESULTS

We observed that both routines give similar results for the considered objective functions, which are highly nonlinear though continuous. There are many local maxima, but one of them is global. For a given starting point only the closest local maximum is located, so computations must usually be repeated to hit the global one. Because the convergence of `fminunc` was far better than that of `fminsearch`, which required much more computation to obtain the same result, we gave up using the latter routine after preliminary tests.

In main experiments, general, LP, and PMI LP PUFBs were examined, with and without the one-regularity conditions satisfied. The number of the sections in a particular factorization, N , was changed from 2 to 8, which corresponds to the filter length L in the range of 8 to 32. The related changes in design freedom depend on the kind of system and are shown in Fig. 3.

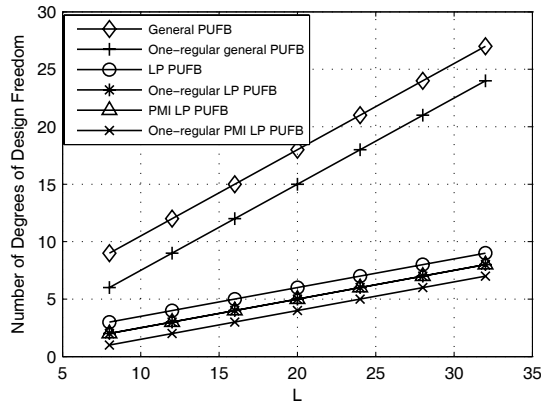


Figure 3: Number of the degrees of design freedom as a function of filter length.

For each combination of the type and length, two thousand filter banks were designed using `fminunc` with different random starting points. Table 1 is the result of a simple analysis of the collected data. The most interesting quantities are also shown in Figures 4 – 6 as functions of filter length.

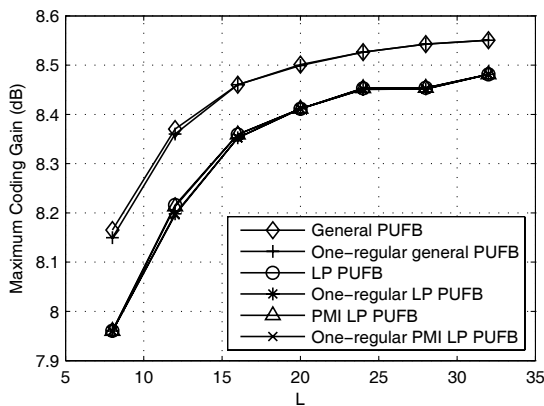


Figure 4: Maximum coding gain as a function of filter length.

Apart from the essential statistical quantities calculated for the obtained coding gains, we are interested in the characteristics of the objective functions. These are the number of the angles to be optimized, the number of the identified local maxima, and the probability of hitting the global maximum. When calculating the latter two quantities, we combined many local maxima into one if the difference between the corresponding coding gains did not exceed 10^{-4} dB, regardless of the angle values. This seemed to be necessary because the coding gain depends only on the magnitude responses of the channel filters, not on their phase responses or order, which are not controlled during the angle optimization. Moreover, neither the coefficients of a hypercomplex lattice structure nor their polar representation are unique when the angles in (24) are unconstrained.

In the case of LP PUFBs, the objective function has a few well distinguishable local maxima, whose number depends linearly on

Table 1: Relation between filter length and maximum coding gain (PHM - probability of hitting the global maximum, NDF - number of the degrees of freedom, NLM - number of local maxima).

L	Obtained coding Gain (dB)					PHM	NDF	NLM
	max	min	mean	median	std. dev.			
General PUFB								
8	8.1653	7.5854	8.1577	8.1653	0.0282	0.8400	9	13
12	8.3702	8.1458	8.3139	8.3122	0.0482	0.3635	12	8
16	8.4604	8.3050	8.4123	8.3977	0.0390	0.2170	15	21
20	8.5010	8.3523	8.4675	8.4744	0.0269	0.1040	18	62
24	8.5265	8.4154	8.5014	8.5059	0.0182	0.0795	21	152
28	8.5428	8.4643	8.5205	8.5252	0.0157	0.0270	24	291
32	8.5508	8.4890	8.5336	8.5369	0.0128	0.0245	28	336
One-regular general PUFB								
8	8.1496	8.1083	8.1292	8.1496	0.0207	0.5050	6	2
12	8.3601	8.1300	8.3040	8.2979	0.0376	0.2305	9	7
16	8.4601	8.2939	8.4193	8.4471	0.0373	0.1325	12	15
20	8.4992	8.3463	8.4690	8.4736	0.0257	0.0750	15	38
24	8.5265	8.3776	8.5021	8.5051	0.0167	0.0150	18	87
28	8.5426	8.4713	8.5231	8.5255	0.0142	0.0385	21	170
32	8.5506	8.4911	8.5372	8.5400	0.0110	0.0380	24	227
LP PUFB								
8	7.9605	6.3979	7.5464	7.9605	0.6898	0.7350	3	2
12	8.2157	6.0275	7.7903	8.2157	0.6417	0.6045	4	4
16	8.3593	5.8353	7.8866	8.2284	0.6909	0.3650	5	6
20	8.4115	5.7245	8.1022	8.3656	0.5948	0.3855	6	9
24	8.4532	5.6567	8.1276	8.4532	0.5300	0.5635	7	14
28	8.4537	5.8239	8.1923	8.4469	0.4700	0.4235	8	20
32	8.4814	5.7366	8.2439	8.4551	0.3995	0.2180	9	27
One-regular LP PUFB								
8	7.9603	6.3924	7.4907	7.9603	0.7183	0.7005	2	2
12	8.1981	6.0217	7.7068	8.1981	0.7262	0.6205	3	4
16	8.3524	5.8300	7.8378	8.2096	0.7065	0.3670	4	6
20	8.4115	5.7196	8.0231	8.3650	0.6642	0.3600	5	9
24	8.4509	5.6521	8.0819	8.4509	0.5886	0.5555	6	14
28	8.4514	5.8060	8.1586	8.4444	0.5074	0.4115	7	20
32	8.4813	5.7217	8.1990	8.4529	0.4365	0.2180	8	24
PMI LP PUFB								
8	7.9601	5.7531	7.3357	7.9601	0.9452	0.6950	2	3
12	8.2131	5.6155	7.7564	8.2131	0.6989	0.6480	3	4
16	8.3591	5.4150	7.9633	8.2282	0.6657	0.3705	4	6
20	8.4115	5.2999	8.0978	8.3650	0.6432	0.3990	5	10
24	8.4531	4.6451	8.1873	8.4531	0.5335	0.6345	6	15
28	8.4537	4.8792	8.2473	8.4469	0.4357	0.4490	7	23
32	8.4813	5.1574	8.2768	8.4551	0.3896	0.2455	8	29
One-regular PMI LP PUFB								
8	7.9599	5.7498	7.3322	7.9599	0.9391	0.6905	1	3
12	8.1958	5.5783	7.7650	8.1958	0.7312	0.7025	2	4
16	8.3522	5.3799	7.8999	8.2094	0.7282	0.3895	3	6
20	8.4115	5.2669	8.0883	8.3644	0.6653	0.3915	4	10
24	8.4509	5.1988	8.1775	8.4509	0.5097	0.6090	5	14
28	8.4514	5.3282	8.2085	8.4444	0.4710	0.4205	6	21
32	8.4813	5.4665	8.2653	8.4528	0.3598	0.2405	7	24

filter length, as Fig. 6 shows. For general PUFB, there is much more maxima and their number grows faster than filter length. Moreover, the differences between the corresponding coding gains are slight.

Regardless of the system, random selection of starting points for line search turns out to guarantee the approaching the global maximum in a moderate number of trials. For general PUFBs, the probability of hitting the maximum is inversely proportional to filter

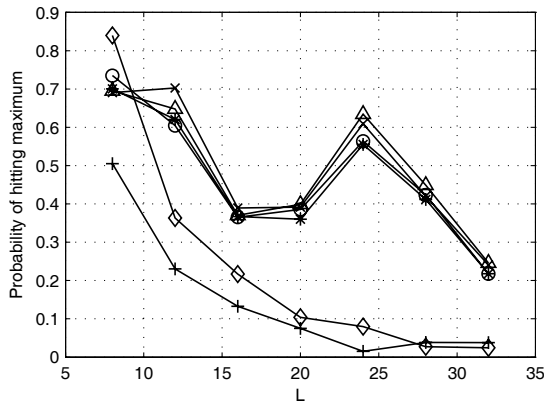


Figure 5: Probability of hitting maximum coding gain as a function of filter length.

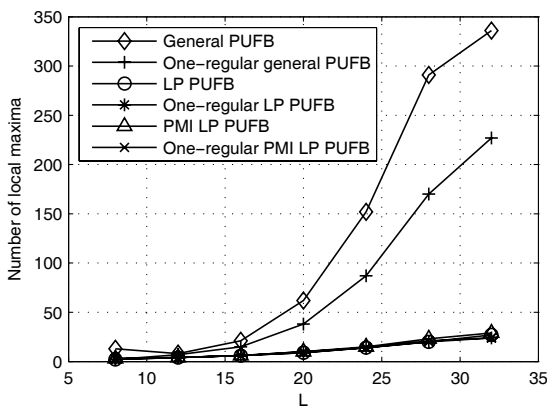


Figure 6: Number of local maxima as a function of filter length.

length and quickly drops. Nevertheless, several dozen of trials are sufficient even for the longest filters. For LP PUFBs only several trials are necessary, and, surprisingly, the increase in filter length does not necessarily decrease the probability. This is shown in Fig. 5.

The linearity of phase responses comes at the cost of decreasing the maximum achievable coding gain, compared with general PUFBs. This is clearly a consequence of the reduction in the number of angles to be optimized, as the coefficients are complex numbers instead of quaternions.

The results concerning the maximum coding gain, obtained for general and LP filter banks, coincide with those reported in [2, 13, 14]. This testifies that the rest of the data is credible. As Fig. 4 shows, the greater filter length, the smaller improvement in coding gain is achieved by adding next stages to the structure.

For both general and LP PUFBs, the one-regularity as well as the PMI symmetry only negligibly affect the maximum achievable coding gain. This is amazing because each of the corresponding constraints eliminates the design freedom related to one hypercomplex lattice coefficient, which is a substantial amount of design freedom, especially for PUFBs with short filters. Thus, the considered properties can be used to make the coefficient synthesis easier, without decreasing the coding performance of the designed filter bank.

6. CONCLUSIONS

In terms of the difficulty of coefficient synthesis and the coding performance of obtained filter banks, quaternionic lattice structures for 4-channel PUFBs are equivalent to the conventional factorizations. Thus, there are good reasons to perform both design and implementation of a filter bank using hypercomplex numbers.

The results reported in literature, concerning the maximum coding gain obtainable for a given filter length, are generally confirmed. However, our observation that in 4-channel PUFBs, the coding gain is only very slightly affected by imposing both one-regularity and the pairwise-mirror-image symmetry of magnitude responses, has the hallmarks of novelty.

The presented method of coefficient synthesis is simple and gives satisfactory results. It allowed us to characterize objective functions in terms of the number of local maxima and the probability of hitting the global maximum.

Both the reported techniques and observations should be interesting and inspiring for persons who contend with filter bank design as well as with other similar optimization problems.

7. ACKNOWLEDGMENTS

This work was supported by the Polish Ministry of Science and Higher Education under the grant N519 030 32/3775.

REFERENCES

- [1] C. W. Kok and T. Q. Nguyen, "Multirate filter banks and transform coding gain," *IEEE Trans. Signal Processing*, vol. 46, no. 7, pp. 2041–2044, 1998.
- [2] A. K. Soman and P. P. Vaidyanathan, "Coding gain in paraunitary analysis/synthesis systems," *IEEE Trans. Signal Processing*, vol. 41, no. 5, pp. 1824–1835, 1993.
- [3] M. Lightstone, E. Majani, and S. K. Mitra, "Low bit-rate design considerations for wavelet-based image coding," *Multi-dimensional Systems and Signal Processing*, vol. 1997, no. 8, pp. 111–128, 1997.
- [4] E. A. B. da Silva and M. Ghanbari, "On the performance of linear phase wavelet transforms in low bit-rate image coding," *IEEE Trans. Image Processing*, vol. 5, no. 5, pp. 689–704, 1996.
- [5] G. Strang and T. Q. Nguyen, *Wavelets and Filter Banks*. Wellesley, MA: Wellesley-Cambridge Press, 1996.
- [6] S. Orantara, T. D. Tran, P. N. Heller, and T. Q. Nguyen, "Lattice structure for regular paraunitary linear-phase filterbanks and m -band orthogonal symmetric wavelets," *IEEE Trans. Signal Processing*, vol. 49, no. 11, pp. 2659–2672, 2001.
- [7] I. L. Kantor and A. S. Solodovnikov, *Hypercomplex Numbers: an Elementary Introduction to Algebras*. New York, NY: Springer, 1989.
- [8] M. Parfieniuk and A. Petrovsky, "Quaternionic lattice structures for four-channel paraunitary filter banks," *EURASIP J. Appl. Signal Process., Special Issue on Multirate Systems and Applications*, vol. 2007, p. 12, 2007, article ID 37481.
- [9] —, "Quaternionic approach to 8-channel general paraunitary filter bank," in *Proc. 13th European Signal Processing Conf. (EUSIPCO)*, Antalya, Turkey, 2005, CD.
- [10] —, "Hypercomplex factorizations for 8-channel linear phase paraunitary filter banks," in *Proc. 7th Int. Conf. and Exhibition "Digital Signal Processing and its Applications" (DSPA)*, vol. 2, Moscow, Russia, 2005, pp. 509–513.
- [11] —, "Quaternionic approach to the one-regular eight-band linear phase paraunitary filter banks," in *Proc. 14th European Signal Processing Conf. (EUSIPCO)*, Florence, Italy, 2006, CD.
- [12] I. The MathWorks, *Matlab Optimization Toolbox User's Guide*, 2006.
- [13] X. Gao, T. Q. Nguyen, and G. Strang, "On factorization of M -channel paraunitary filterbanks," *IEEE Trans. Signal Processing*, vol. 49, no. 7, pp. 1433–1446, 2001.
- [14] J. Liang, T. D. Tran, and R. L. De Queiroz, "DCT-based general structure for linear phase paraunitary filter banks," *IEEE Trans. Signal Processing*, vol. 51, no. 6, pp. 1572–1580, 2003.